

RESEARCH ARTICLE | OCTOBER 28 2021

Disordered metamaterial coating for daytime passive radiative cooling

Bhrigu Rishi Mishra  ; Sreerag Sundaram  ; Nithin Jo Varghese; Karthik Sasihithlu  

 Check for updates

AIP Advances 11, 105218 (2021)

<https://doi.org/10.1063/5.0064572>



AIP Advances
Special Topic: Machine Vision,
Optical Sensing and Measurement

Submit Today

 AIP
Publishing

Disordered metamaterial coating for daytime passive radiative cooling

Cite as: AIP Advances 11, 105218 (2021); doi: 10.1063/5.0064572

Submitted: 19 August 2021 • Accepted: 4 October 2021 •

Published Online: 28 October 2021



View Online



Export Citation



CrossMark

Bhrigu Rishi Mishra, Sreerag Sundaram, Nithin Jo Varghese, and Karthik Sasihithlu^{a)}

AFFILIATIONS

Department of Energy Science and Engineering, Indian Institute of Technology Bombay, Powai, Mumbai 400076, Maharashtra, India

^{a)}Author to whom correspondence should be addressed: ksasihithlu@ese.iitb.ac.in

ABSTRACT

In this theoretical study, a disordered metamaterial coating with randomly embedded TiO₂ dielectric microspheres in a polydimethylsiloxane matrix has been designed for the purpose of daytime passive radiative cooling. While retaining the necessary optical properties of high reflectivity ($\approx 94\%$) in the solar spectrum and high emissivity ($\approx 96\%$) in the atmospheric transparency window, the coating exhibits the following additional desirable properties: (a) low volume fraction of TiO₂ microspheres, ensuring minimal possibility of agglomeration of particles during fabrication; and (b) a cooling power of 81.8 W/m^2 , which is among the highest for similar coatings that have been developed. We also show how a modified form of Kubelka–Munk theory with empirical relations originally developed to analyze optical scattering in biological tissue layers can be used for designing radiative cooling structures. The predictions from this method have been validated using Monte Carlo simulations. It is expected that this study will motivate further similar designs in the rapidly expanding market for effective and easy-to-fabricate coatings for daytime passive radiative cooling applications.

© 2021 Author(s). All article content, except where otherwise noted, is licensed under a Creative Commons Attribution (CC BY) license (<http://creativecommons.org/licenses/by/4.0/>). <https://doi.org/10.1063/5.0064572>

01 July 2024 02:40:52

I. INTRODUCTION

Passive radiative cooling is an effective way to reduce the heating of the space without consuming electricity.¹ This technique utilizes the transparency of the atmosphere in the $8\text{--}13 \mu\text{m}$ wavelength range (also called the atmospheric transparency window). A coating with high reflectivity in the solar spectrum and high emissivity in this atmospheric transparency window, when coated on the exterior walls of an enclosure, can cool the interior space by reflecting incident solar radiation and dissipating heat into space in the atmospheric transparency window. An ideal radiative cooler with unit emissivity in the atmospheric transparency window, unit reflectivity elsewhere, and zero nonradiative heat loss has been theoretically shown to cool enclosing space by as much as 60°C below the ambient.² Several attempts carried out over the last decade to realize this experimentally have been aptly summarized in a recent review.³ In order to achieve high solar reflection, a thin film of silver coating has been utilized in many of these works.^{1,4,5} In addition, a majority of these works^{4,6,7} adopt a double-layer coating for daytime passive radiative cooling, one for achieving high reflection and the other for high emissivity.

In recent works,^{6–9} Mie scattering from dielectric particles embedded in a coating has been utilized to achieve high solar reflection. Atiganyanun *et al.*⁹ showed that a photonic random media containing a high volume fraction of low refractive index dielectric spheres exhibits high reflection in the solar spectrum due to minimization of the photon transport mean-free path. However, employing a high volume fraction of particles runs the risk of agglomeration of these particles, thereby altering the optical properties of the structure.¹⁰ Instead of using low refractive index spheres with high volume fraction, high refractive index particles (such as TiO₂) with low volume fraction can also be used to achieve high reflection in the solar spectrum.^{6–8} However, obtaining high reflection ($>90\%$) while maintaining low volume fraction (around 5%–8%) of TiO₂ spherical particles, as has been carried out in these works, will require a substantial increase in thickness of the coating, which leads to reduced cooling power of the coating due to increased solar absorption losses as well as an increase in nonradiative heat losses.

In this work, we have designed a metamaterial coating consisting of monodisperse TiO₂ microspheres randomly embedded in the polydimethylsiloxane (PDMS) matrix that gives both the desired optical properties necessary for daytime passive radiative cooling in

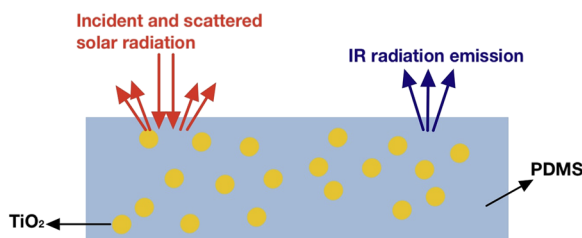


FIG. 1. Schematic of the designed disordered metamaterial. TiO_2 spherical particles scatter incident solar radiation, and the PDMS matrix gives high emissivity in the atmospheric transparency window.

a single-layer coating. In addition, we have ensured that an optimal combination of the volume fraction and thickness of the coating is maintained such that not only is the possibility of agglomeration of particles minimized but the thickness of the metamaterial is such that solar absorption losses and the nonradiative heat losses are also low. This we show increases the cooling power of the coating substantially.

For our coating, the schematic of which is shown in Fig. 1, we have chosen PDMS as the background matrix. PDMS is a widely used organic polymer that exhibits a multitude of desirable properties, including low cost, biocompatibility, heat and moisture resistance, and chemical inertness.¹¹ In addition, PDMS is highly transparent in the solar spectrum and highly absorbing (emissive) in the infrared region, which results in high emissivity in the atmospheric transparency window.^{5,12} The high reflectivity of the coating in the solar spectrum comes about from the scattering of incoming radiation by the TiO_2 microspheres embedded in the PDMS matrix whose radii are chosen such that their scattering efficiency is high for that wavelength range. In addition to high cooling power, the advantages of the present design are its simplicity, cost effectiveness, and ease of fabrication. The use of thin metal coating employed in other works to obtain high solar reflection is avoided here as its presence can be visually unappealing¹² due to its mirror-like finish and difficulty in deployment due to the requirement of multiple layers to achieve passive radiative cooling. The present coating not just exhibits diffuse reflection and hence visually desirable but is designed to be a single-layer coating and hence easier to fabricate and deploy. In addition to the excellent optical properties necessary for passive radiative cooling, PDMS/ TiO_2 coating is highly stable, hydrophobic, and biocompatible.¹³ Even though TiO_2 is known to absorb in the ultraviolet regime,^{14,15} mainly in the UVC (100–280 nm) and UVB (280–315 nm) bands, since almost all the incident radiation in the UVC and UVB bands is blocked by the Earth's ozone layer and atmosphere, chances of photo-degradation of TiO_2 upon exposure to the environment are significantly reduced. Moreover, it has been recently demonstrated¹⁶ that PDMS is able to suppress the photo-degradation of TiO_2 particles even further. This has enabled the use of the PDMS– TiO_2 composite for various outdoor applications with negligible to no photo-degradation being reported.^{13,16–19}

II. METHOD FOR CHARACTERIZING THE OPTICAL PROPERTIES OF THE COATING

For the design process, the optical properties of the coating can be obtained using exact electromagnetic solvers. However, especially

in the high frequency regime (such as that in the solar spectrum) when the thickness of the coating with random inclusions is a few hundreds of micrometers, using exact numerical solvers becomes computationally prohibitive. In such regimes and when the volume fraction of scatterers is low enough such that near-field interaction between particles can be neglected, optical scattering from random media can be analyzed by solving the radiative transfer equation using the Monte Carlo (MC) simulation technique. Indeed, several recent works^{7,8,20} on radiative cooling have adopted MC simulation to obtain the optical properties such as reflectivity and transmissivity of the designed structures. However, these simulation techniques do not throw clarity on the interplay between parameters, which would result in the desired optical properties. It would thus be desirable to explore alternate analytical techniques, which are not just effective to analyze the properties but which would also throw clarity on the interplay between parameters and hence can be used to find the optimal combination of parameters for the structure.

Here, we adopt Kubelka–Munk (KM) theory²¹ to find the optimal combination of the design parameters, viz., radius of spherical particles (r), their volume fraction (f), and thickness (L) of the coating for radiative cooling to be effective.

A. Kubelka–Munk theory with modified coefficients

The Kubelka–Munk (KM) two-flux radiative transfer model²¹ is a simple yet effective approach to describe optical properties of inhomogenous media and one that does not require much computational effort. This theory is frequently used to calculate reflectivity and absorptivity of pigment films.^{22,23} However, to the best knowledge of the authors, this method has not been used in the design of a radiative cooling coating. Atiganyanun *et al.*⁹ have employed this theory to calculate the photon transport mean free path but have not employed this to obtain the optical parameters. Here, we employ KM theory to design the coating to achieve maximum reflection in the solar spectrum. This region is particularly important since studies have shown that it is necessary for the coating to have >95% reflection to effectively nullify²⁴ daytime heating from the sun. The expression for the reflectance R from KM theory is given by²³

$$R = \frac{(1 - \gamma)(1 + \gamma)(\exp(AL) - \exp(-AL))}{(1 + \gamma)^2 \exp(AL) - (1 - \gamma)^2 \exp(-AL)}, \quad (1)$$

where L is the thickness of the layer and the coefficients γ and A are given by $\gamma = \sqrt{K/(K + 2S)}$ and $A = \sqrt{K(K + 2S)}$. Here, K and S are the absorption and scattering coefficients, respectively. In the independent scattering regime, they can be calculated using Mie theory as²²

$$K = \frac{3fQ_{\text{abs}}}{4r}, \quad S = \frac{3fQ_{\text{sca}}}{4r}, \quad (2)$$

where f is the volume fraction, r is the radius of the sphere, and Q_{abs} (Q_{sca}) is the absorption (scattering) efficiency of a single dielectric sphere calculated from Mie theory. In the limit of low absorption $KL \rightarrow 0$, the reflectance in Eq. (1) can be shown to reduce to²¹

$$R = \frac{SL}{SL + 1}. \quad (3)$$

KM theory when applied using the coefficients from Eq. (2) has several limitations. The derivation of optical properties such as

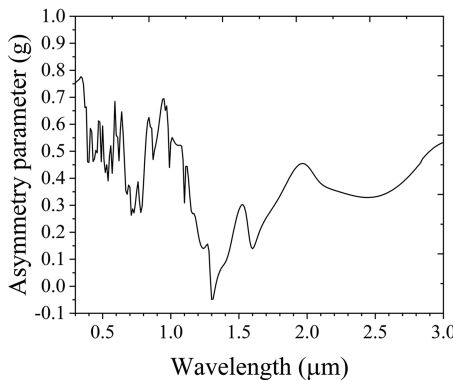


FIG. 2. Asymmetry parameter (g) of the TiO_2 spherical particle with a radius of $0.6 \mu\text{m}$.

reflectance in Eq. (1) assumes incident radiation to be diffuse, does not account for reflection at the boundaries, and considers isotropic scattering by the particles. However, sunlight incident on the coating is collimated; the change in the refractive index at the boundaries can cause significant losses due to reflection; and the Mie scattering asymmetry parameter g^{25} for TiO_2 microspheres has a value greater than zero in the solar spectrum, indicating enhanced forward scattering (Fig. 2) and thereby deviation from the isotropic scattering model ($g = 0$). Hence, the coefficients from Eq. (2) cannot be used as is without significant errors. We thus modify the coefficients as follows: for anisotropic particles, the scattering efficiency is reduced by a factor $(1 - g)$ so that the reduced scattering efficiency^{26,27} is given by $S' = 3fQ_{\text{sca}}(1 - g)/(4r)$. As has been explained in Ref. 26, this factor $(1 - g)$ accounts for the altered mean-free path of the photons when $g > 0$ compared to the isotropic scattering case. While this expression for S' accounts for the anisotropic nature of scattering, the presence of collimated light and losses due to reflection at the boundaries of the coating is still unaccounted. These can be accounted for by modifying the coefficients from Eq. (2) using the empirical relations from Roy *et al.*²⁸ who have derived these for analyzing the optical properties of biological tissues. The modified coefficients K_{emp} and S_{emp} (in mm^{-1}) read

$$K_{\text{emp}} = K + 2.43(KS')^{0.72}, \quad (4)$$

$$S_{\text{emp}} = 0.408 S' \quad (5)$$

and are employed in Eq. (1) to characterize the optical properties of the coating in the solar spectrum.

B. Size parameters for the coating

The relations in Eqs. (4) and (5), where the scattering coefficient is expressed in terms of scattering properties of a single particle, have been obtained for low volume fraction conditions in the independent scattering regime.²⁹ Employing these coefficients from Eqs. (4) and (5) to find the optical parameters such as reflectivity from Eq. (3) thus requires us to operate in a similar regime. As per the limits of independent scattering approximation,³⁰ the volume fraction f should be less than 0.27 and the ratio of interparticle spacing c to

wavelength λ should be greater than 0.3. Since these parameters are related to one another via the empirical relation³¹

$$c = 2r \left(\frac{0.905}{f^{1/3}} - 1 \right), \quad (6)$$

this allows us to arrive at the appropriate values of parameters r and f for Eqs. (4) and (5) to be valid. We observe that the values $r = 600 \text{ nm}$ and $f = 0.15$ satisfy these required conditions over a large part of the solar spectrum $0.2 \mu\text{m} < \lambda < 2.8 \mu\text{m}$ while also ensuring that the thickness of the layer to achieve $\gtrsim 0.95$ reflection in this wavelength range is minimized. We use these optimized values of r and f to calculate the reflectivity of the disordered metamaterial using KM theory. In order to obtain high reflectance ($\gtrsim 95\%$) over the solar spectrum, which is crucial for minimizing daytime heating from the sun, we analyze its dependence on the thickness of the metamaterial layer. As the thickness of metamaterial increases, the number of scatterers also increases, which directly enhances multiple scattering of incident radiation and in turn translates to high reflectance. The reflectivity of the metamaterial is calculated for varying sample thicknesses and plotted in Fig. 3. It is seen that reflectivity increases sharply until $500 \mu\text{m}$ and is nearly constant for larger thicknesses. We thus retain $500 \mu\text{m}$ as the thickness of the sample for our calculation.

C. Characterizing the optical properties of the coating in IR region

While KM theory with coefficients given by Eqs. (4) and (5) is applicable for the wavelength range in the solar spectrum, it cannot be used for higher wavelengths since the ratio c/λ reduces below the limit of 0.3 where dependent scattering arising due to interference effects in the field from different scatterers starts to become important. Here, the scattering coefficient S' can no longer be trivially expressed in terms of scattering efficiency of a single particle and use of exact electromagnetic solvers to accurately analyze the scattered field from the coating is necessary. We have thus modeled the optical properties of the metamaterial in the IR region using the commercial electromagnetic solver CST microwave studio. The refractive index data of TiO_2 and PDMS are obtained from

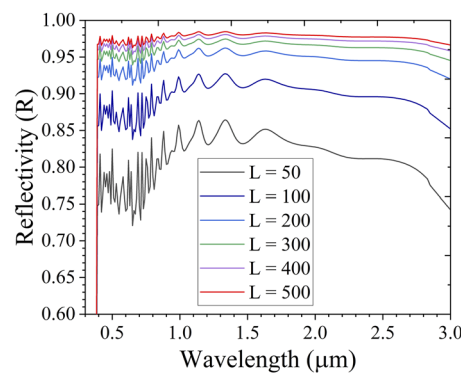


FIG. 3. Reflectivity of the coating for various thicknesses calculated using KM theory. Here, thickness L is in micrometers.

Palik³² and Zhang *et al.*,^{33,34} respectively. The frequency domain solver with unit cell boundary conditions has been used for the simulation.

III. RESULTS AND DISCUSSION

A. Broadband reflectance, emittance, and comparison with Monte Carlo simulations

One of the advantages of using disordered metamaterial structures is that unlike ordered metamaterial where high reflectivity is achieved only at resonance frequencies,³⁵ in disordered metamaterial, broadband reflectivity is possible. The broadband width over which disordered metamaterial is reflective depends on the wavelength range over which the dielectric sphere has high scattering efficiency, which from Eq. (5) translates to high scattering coefficient for the metamaterial layer. The scattering coefficient S_{emp} for the layer with TiO_2 spherical particles of $r = 0.6 \mu\text{m}$ and $f = 0.15$ is plotted in Fig. 4. The multiple peaks in Fig. 4, which are distributed over the entire solar spectrum, correspond to the resonances of the TiO_2 sphere of radius $0.6 \mu\text{m}$. The presence of these resonance peaks over the entire solar spectrum thus results in high reflection over this entire wavelength range as shown in Fig. 5. The average reflectivity calculated as $R_{\text{avg}} = \int I_{\text{AM1.5}}(\lambda)R(\lambda)d\lambda / \int I_{\text{AM1.5}}(\lambda)d\lambda$, where $I_{\text{AM1.5}}(\lambda)$ is the spectral solar irradiance,³⁶ over the solar spectrum, i.e., $0.3\text{--}3 \mu\text{m}$, is observed to be 0.94. The absorption peak around $0.3 \mu\text{m}$ for the TiO_2 material in fact reduces the overall reflection in the solar spectrum, and if techniques can be developed to scatter radiation around $0.3 \mu\text{m}$, the reflectivity of the metamaterial in the solar spectrum increases to ≈ 0.97 .

The reflectivity plots obtained using KM theory are verified by comparing with data from MC simulations. The MC technique^{37,38} is a stochastic method that models the propagation of each injected photon propagation as a random walk and uses ensemble average of a large number of photons to obtain the physical quantity of interest. Its statistical nature is what has prompted it to be considered as the gold standard in validating other studies.³⁸ Here, we use the MC computational code developed by Wang *et al.*³⁷ for the reflectivity calculation. The comparison between reflectivity plots of KM theory and that obtained from MC simulation is shown in Fig. 5. The plots show a good match, confirming the predictions of KM theory with the modified coefficients.

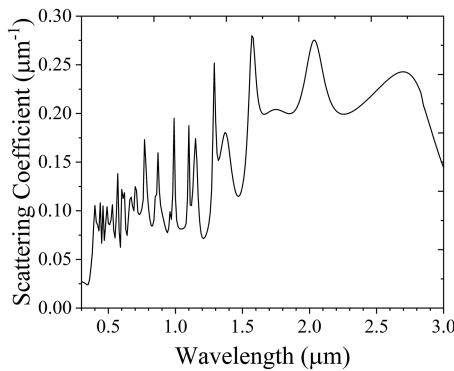


FIG. 4. Scattering coefficient (S_{emp}) of the designed disordered metamaterial.

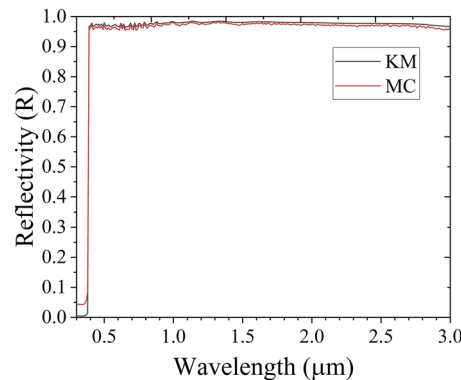


FIG. 5. Comparison between reflectivity values calculated using KM theory and MC simulations for a $500 \mu\text{m}$ thick sample.

The emissivity spectrum in the IR region obtained from the CST microwave studio is shown in Fig. 6. The average emissivity in IR ($6\text{--}15 \mu\text{m}$) calculated as $\varepsilon_{\text{avg}} = \int I_{\text{AM1.5}}(\lambda)\varepsilon(\lambda)d\lambda / \int I_{\text{AM1.5}}(\lambda)d\lambda$ is observed to be 0.96. Recently,⁴ it has been shown that the presence of Fröhlich resonances in dielectric spheres²⁵ can be exploited to obtain high emissivity of composite structures in the atmospheric transparency window region. It is thus of interest to see whether the high emissivity in the IR region observed in this work is a result of Fröhlich resonances of the TiO_2 microspheres. To explore this, we plot the emission spectrum of a bare $500 \mu\text{m}$ thick PDMS block (without any embedded dielectric particles) in Fig. 7(a) and the absorption efficiency Q_{abs} of a TiO_2 spherical particle of radius 600 nm in Fig. 7(b). Comparing Figs. 6 and 7(a), we observe that the high emissivity in the IR region of the PDMS/ TiO_2 composite is mainly due to high absorptive nature of PDMS material. Minor deviations are observed in the $6\text{--}8 \mu\text{m}$ wavelength range and are due to scattering by TiO_2 microspheres. Moreover, the absorption efficiency of TiO_2 microspheres, shown in Fig. 7(b), is close to zero in the $8\text{--}12 \mu\text{m}$ wavelength range and peaks at $14.1 \mu\text{m}$. This absorption peak arising due to the presence of Fröhlich resonance will thus have

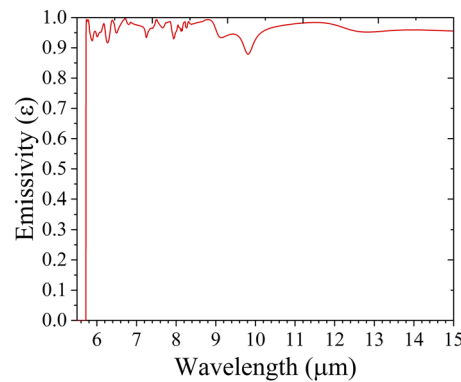


FIG. 6. Emissivity of the disordered metamaterial in the IR region modeled using CST microwave studio.

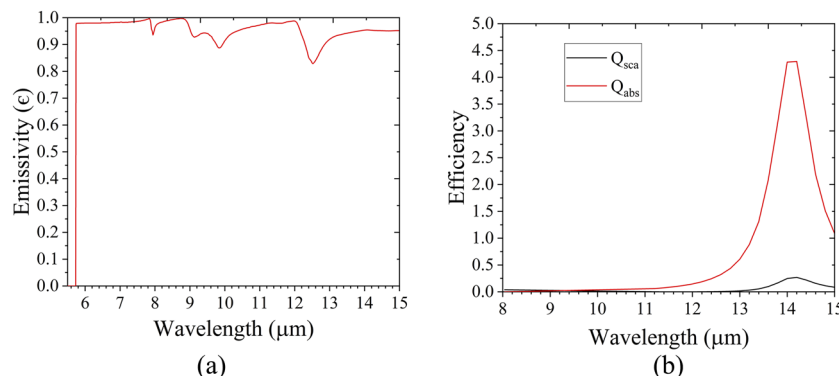


FIG. 7. (a) Emissivity of a 500 μm thick PDMS block. (b) Scattering (Q_{sca}) and absorption (Q_{abs}) efficiency of the TiO_2 sphere of radius 600 nm in the 8–15 μm wavelength region in free space.

negligible contribution to the emissivity of the PDMS/ TiO_2 coating in the atmospheric transparency window.

B. Calculation of cooling power and comparison with other works

Using the optical properties of the coating determined over the visible and IR spectra, we can now calculate its net cooling power to show its effectiveness for passive daytime cooling applications. The cooling power (P_{net}) can be expressed in terms of the power radiated from the coating (P_{rad}), power absorbed by the coating due to incident solar radiation (P_{sun}), the incident atmospheric radiation (P_{atm}), and the conduction and convection heat losses to the surroundings ($P_{\text{cond+conv}}$) as

$$P_{\text{net}} = P_{\text{rad}} - P_{\text{sun}} - P_{\text{atm}} - P_{\text{cond+conv}}, \quad (7)$$

where, considering solar radiation to be incident normal to the coating and emitted radiation by the coating and the atmosphere taken to be isotropic, we will have

$$P_{\text{rad}} = A\pi \int_0^{\infty} \epsilon(\lambda) I_{\text{bb}}(T, \lambda) d\lambda, \quad (8)$$

$$P_{\text{sun}} = A \int_0^{\infty} \epsilon(\lambda) I_{\text{AM1.5}}(\lambda) d\lambda, \quad (9)$$

$$P_{\text{atm}} = A\pi \int_0^{\infty} \epsilon(\lambda) \epsilon_{\text{atm}}(\lambda) I_{\text{bb}}(T_{\text{amb}}, \lambda) d\lambda, \quad (10)$$

$$P_{\text{cond+conv}} = Ah(T_{\text{amb}} - T). \quad (11)$$

Here, $\epsilon(\lambda)$ is the emissivity of the metamaterial (shown in Fig. 6), ϵ_{atm} is the emissivity of the atmosphere that is given by $\epsilon_{\text{atm}} = 1 - \tau^{1/\cos\theta}$ (where τ is the atmospheric transmittance³⁹ and θ (taken to be zero for this work) is the angle of incidence), $I_{\text{bb}}(T, \lambda)$ is the spectral blackbody radiation at the coating temperature T , T_{amb} is the surrounding temperature, A is the area of the metamaterial, and h is the overall heat transfer coefficient of the metamaterial coating. Whatever is transmitted from the coating is assumed to be absorbed by the substrate below. This assumption would thus give the lower limit for the cooling power since any reflection of radiation from the substrate below would only add on to it.

A comparison of optical properties (R and ϵ) and cooling power of the present coating with other similar works where random media of TiO_2 is used as a reflector^{6,7} is summarized in Tables I and II, respectively. Details of different components of the cooling power from Eqs. (8)–(11) are also given in Table II. It can be seen from Table I that the reflectivity of disordered metamaterial coating is higher than that in other works due to which our coating has lowest solar absorption losses (Table II). We have used emission spectra provided in the Refs. 6 and 7 to calculate the individual components in Eq. (7). The ambient temperature (T_{amb}) and coating temperature (T) are taken to be the same and at 27 °C so that losses due to $P_{\text{cond+conv}}$ will be negligible. The net cooling power of present coating is seen to be significantly larger compared to other works due to both minimal absorption in the solar spectrum and high emissivity in the 6–15 μm region.

TABLE I. Comparison of reflectivity (R) and emissivity (ϵ) of disordered metamaterial with other works in solar spectrum and atmospheric transparency window, respectively.

Work	R (0.3–3 μm)	ϵ (8–13 μm)
This work	0.94	0.96
Huang and Ruan (2017) ⁷	0.92	0.96
Bao <i>et al.</i> (2017) ⁶ (TiO_2+SiC)	0.9	0.93
Bao <i>et al.</i> (2017) ⁶ ($\text{TiO}_2+\text{SiO}_2$)	0.9	0.9

TABLE II. Comparison of different cooling power components of disordered metamaterial with other works.

Work	P_{net}	P_{rad}	P_{atm}	P_{sun}	Substrate
This work	81.8	214.2	70.8	61.6	Black
Huang and Ruan (2017) ⁷	59.8	225.0	76.4	88.8	Black
Bao <i>et al.</i> (2017) ⁶ (TiO_2+SiC)	59.5	211.3	69.0	82.8	Aluminum
Bao <i>et al.</i> (2017) ⁶ ($\text{TiO}_2+\text{SiO}_2$)	49.7	165.9	39.4	76.8	Aluminum

IV. CONCLUSION

We have designed a coating consisting of TiO₂ microspheres randomly embedded in the PDMS matrix that simultaneously gives high solar reflection and high emission in the atmospheric transparency window. We have also shown how KM theory with modified absorption and scattering coefficients whose empirical relations were initially developed to analyze optical scattering in biological tissues can be effectively employed to analyze optical properties of radiative cooling coatings. The results from KM theory have been confirmed using MC simulations. The designed metamaterial coating is observed to have a reflectivity of 0.94 in the solar spectrum and an emissivity of 0.96 in the atmospheric transparency window. The calculated cooling power of 81.8 W/m² of the designed metamaterial is a significant improvement over previous works where TiO₂ spheres have been used to obtain diffuse reflection in the solar spectrum. The results from this work are expected to spur further improvements in the design of single-layer coatings with monodisperse inclusions which are easier to fabricate and deploy compared to multi-layer coatings.

ACKNOWLEDGMENTS

B.R.M. acknowledges support from Prime Minister's Research Fellowship (PMRF). K.S. acknowledges support from La Fondation Dassault Systèmes and SERB Grant No. SRG/2020/001 511.

AUTHOR DECLARATIONS

Conflict of Interest

The authors have no conflicts to disclose.

DATA AVAILABILITY

The data that support the findings of this study are available from the corresponding author upon reasonable request.

REFERENCES

- ¹A. P. Raman, M. A. Anoma, L. Zhu, E. Rephaeli, and S. Fan, "Passive radiative cooling below ambient air temperature under direct sunlight," *Nature* **515**, 540–544 (2014).
- ²Z. Chen, L. Zhu, A. Raman, and S. Fan, "Radiative cooling to deep sub-freezing temperatures through a 24-h day-night cycle," *Nat. Commun.* **7**, 13729 (2016).
- ³B. Zhao, M. Hu, X. Ao, N. Chen, and G. Pei, "Radiative cooling: A review of fundamentals, materials, applications, and prospects," *Appl. Energy* **236**, 489–513 (2019).
- ⁴Y. Zhai, Y. Ma, S. N. David, D. Zhao, R. Lou, G. Tan, R. Yang, and X. Yin, "Scalable-manufactured randomized glass-polymer hybrid metamaterial for daytime radiative cooling," *Science* **355**, 1062–1066 (2017).
- ⁵J.-l. Kou, Z. Jurado, Z. Chen, S. Fan, and A. J. Minnich, "Daytime radiative cooling using near-black infrared emitters," *ACS Photonics* **4**, 626–630 (2017).
- ⁶H. Bao, C. Yan, B. Wang, X. Fang, C. Y. Zhao, and X. Ruan, "Double-layer nanoparticle-based coatings for efficient terrestrial radiative cooling," *Sol. Energy Mater. Sol. Cells* **168**, 78–84 (2017).
- ⁷Z. Huang and X. Ruan, "Nanoparticle embedded double-layer coating for daytime radiative cooling," *Int. J. Heat Mass Transfer* **104**, 890–896 (2017).
- ⁸J. Peoples, X. Li, Y. Lv, J. Qiu, Z. Huang, and X. Ruan, "A strategy of hierarchical particle sizes in nanoparticle composite for enhancing solar reflection," *Int. J. Heat Mass Transfer* **131**, 487–494 (2019).
- ⁹S. Atiganyanun, J. B. Plumley, S. J. Han, K. Hsu, J. Cytrynbaum, T. L. Peng, S. M. Han, and S. E. Han, "Effective radiative cooling by paint-format microsphere-based photonic random media," *ACS Photonics* **5**, 1181–1187 (2018).
- ¹⁰L. Ma, C. Wang, and L. Liu, "Polarized radiative transfer in dense dispersed media containing optically soft sticky particles," *Opt. Express* **28**, 28252–28268 (2020).
- ¹¹D. Ghosh and D. Khastgir, "Degradation and stability of polymeric high-voltage insulators and prediction of their service life through environmental and accelerated aging process," *ACS Omega* **3**, 11317–11330 (2018).
- ¹²T. Suichi, A. Ishikawa, T. Tanaka, Y. Hayashi, and K. Tsuruta, "Whitish daytime radiative cooling using diffuse reflection of non-resonant silica nanoshells," *Sci. Rep.* **10**, 6486 (2020).
- ¹³Y. Wang, Z. Huang, R. S. Gurney, and D. Liu, "Superhydrophobic and photocatalytic PDMS/TiO₂ coatings with environmental stability and multifunctionality," *Colloids Surf., A* **561**, 101–108 (2019).
- ¹⁴C.-S. Jwo, D.-C. Tien, T.-P. Teng, H. Chang, T.-T. Tsung, C. Y. Liao, and C.-H. Lin, "Preparation and UV characterization of TiO₂ nanoparticles synthesized by Sanss," *Rev. Adv. Mater. Sci.* **10**, 283–288 (2005).
- ¹⁵J. Xu, L. Li, Y. Yan, H. Wang, X. Wang, X. Fu, and G. Li, "Synthesis and photoluminescence of well-dispersible anatase TiO₂ nanoparticles," *J. Colloid Interface Sci.* **318**, 29–34 (2008).
- ¹⁶R. L. Upton and C. R. Crick, "Pigmented self-cleaning coatings with enhanced UV resilience via the limitation of photocatalytic activity and its effects," *Mol. Syst. Des. Eng.* **5**, 876–881 (2020).
- ¹⁷R. Hickman, E. Walker, and S. Chowdhury, "TiO₂-PDMS composite sponge for adsorption and solar mediated photodegradation of dye pollutants," *J. Water Process Eng.* **24**, 74–82 (2018).
- ¹⁸J. Labille, J. Feng, C. Botta, D. Borschneck, M. Sammut, M. Cabie, M. Auffan, J. Rose, and J.-Y. Bottero, "Aging of TiO₂ nanocomposites used in sunscreen: dispersion and fate of the degradation products in aqueous environment," *Environ. Pollut.* **158**, 3482–3489 (2010).
- ¹⁹D. T. Vaimakis-Tsogkas, D. G. Bekas, T. Giannakopoulou, N. Todorova, and A. S. Paipetis, "Effect of TiO₂ addition/coating on the performance of polydimethylsiloxane based silicone elastomers for outdoor applications," *Mater. Chem. Phys.* **223**, 366–373 (2019).
- ²⁰Z. Cheng, F. Wang, H. Wang, H. Liang, and L. Ma, "Effect of embedded polydisperse glass microspheres on radiative cooling of a coating," *Int. J. Thermal Sci.* **140**, 358–367 (2019).
- ²¹P. Kubelka, "New contributions to the optics of intensely light scattering materials. Part I," *J. Opt. Soc. Am.* **38**, 448–457 (1948).
- ²²M. K. Gunde and Z. C. Orel, "Absorption and scattering of light by pigment particles in solar-absorbing paints," *Appl. Opt.* **39**, 622–628 (2000).
- ²³M. Quinten, "The color of finely dispersed nanoparticles," *Appl. Phys. B* **73**, 317–326 (2001).
- ²⁴M. Gali, M. Arnold, A. Gentle, and G. Smith, "Super-cool paints: Optimizing composition with a modified four-flux model," *Proc. SPIE* **10369**, 103690A-1–103690A-10 (2017).
- ²⁵C. F. Bohren and D. R. Huffman, *Absorption and Scattering of Light by Small Particles* (John Wiley & Sons, 2008).
- ²⁶L. F. Gate, "The determination of light absorption in diffusing materials by a photon diffusion model," *J. Phys. D: Appl. Phys.* **4**, 1049–1056 (1971).
- ²⁷B. J. Brinkworth, "Interpretation of the Kubelka-Munk coefficients in reflection theory," *Appl. Opt.* **11**, 1434–1435 (1972).
- ²⁸A. Roy, R. Ramasubramanian, and H. A. Gaonkar, "Empirical relationship between Kubelka-Munk and radiative transfer coefficients for extracting optical parameters of tissues in diffusive and nondiffusive regimes," *J. Biomed. Opt.* **17**, 115006 (2012).
- ²⁹L. Tsang, J. A. Kong, and K. H. Ding, *Scattering of Electromagnetic Waves: Theories and Applications* (John Wiley & Sons, Inc., 2000).
- ³⁰H. C. Hottel and A. F. Sarofim, "Optical properties of coatings. Effect of pigment concentration," *AIAA J.* **9**, 1895–1898 (1971).
- ³¹M. Q. Brewster and C. L. Tien, "Radiative transfer in packed fluidized beds: Dependent versus independent scattering," *J. Heat Transfer* **104**, 573–579 (1982).
- ³²E. D. Palik, *Handbook of Optical Constants of Solids* (Academic Press, 1998).
- ³³X. Zhang, J. Qiu, X. Li, J. Zhao, and L. Liu, "Complex refractive indices measurements of polymers in visible and near-infrared bands," *Appl. Opt.* **59**, 2337–2344 (2020).

- ³⁴X. Zhang, J. Qiu, J. Zhao, X. Li, and L. Liu, "Complex refractive indices measurements of polymers in infrared bands," *J. Quant. Spectrosc. Radiat. Transfer* **252**, 107063 (2020).
- ³⁵Y. Huang, H. Xu, Y. Lu, and Y. Chen, "All-dielectric metasurface for achieving perfect reflection at visible wavelengths," *J. Phys. Chem. C* **122**, 2990–2996 (2018).
- ³⁶ASTM International, ASTM G173-03, Standard Tables for Reference Solar Spectral Irradiances: Direct Normal and Hemispherical on 37° Tilted Surface, 2012.
- ³⁷L. Wang, S. L. Jacques, and L. Zheng, "MCML—Monte Carlo modelling of light transport in multi-layered tissues," *Comput. Methods Programs Biomed.* **47**, 131–146 (1995).
- ³⁸L. Wang, S. Ren, and X. Chen, "Comparative evaluations of the Monte Carlo-based light propagation simulation packages for optical imaging," *J. Innovative Opt. Health Sci.* **11**, 1750017 (2018).
- ³⁹A. R. Gentle and G. B. Smith, "Radiative heat pumping from the earth using surface phonon resonant nanoparticles," *Nano Lett.* **10**, 373–379 (2010).